Chemistry
A European
Journal

Chemistry Europe
European Chemical Societies Publishing

Accepted Article

Title: Five-Step Enantioselective Synthesis of Islatravir via Asymmetric Ketone Alkynylation and an Ozonolysis Cascade

Authors: Aaron Whittaker, Niki R. Patel, Mark A. Huffman, Xiao Wang, Bangwei Ding, Mark McLaughlin, Justin A. Newman, Teresa Andreani, Kevin M. Maloney, and Heather C. Johnson

To be cited as: *Chem. Eur. J.* 10.1002/chem.202003091

Link to VoR: https://doi.org/10.1002/chem.202003091

WILEY-VCH

10.1002/chem.202003091

RESEARCH ARTICLE

WILEY-VCH

Five-Step Enantioselective Synthesis of Islatravir via Asymmetric Ketone Alkynylation and an Ozonolysis Cascade

Niki R. Patel, Mark A. Huffman, Xiao Wang, Bangwei Ding, Mark McLaughlin, Justin A. Newman, Teresa Andreani, Kevin M. Maloney, Heather C. Johnson* and Aaron M. Whittaker*

N. R. Patel, M. A. Huffman, X. Wang, B. Ding, M. McLaughlin, J. Newman, T. Andreani, K. M. Maloney, H. C. Johnson and A. M. Whittaker
Department of Process Research and Development, MRL, Merck & Co., Inc., Rahway, NJ 07065 USA
[*] Correspondence to aaron.whittaker@merck.com and heather.johnson@merck.com

Supporting information for this article is given via a link at the end of the document.

Abstract: A 5-step enantioselective synthesis of the potent anti-HIV nucleoside islatravir is reported. The highly efficient route was enabled by a novel enantioselective alkynylation of an *α,β*-unsaturated ketone, a unique ozonolysis-dealkylation cascade in water, and an enzymatic aldol-glycosylation cascade.

Introduction

According to the World Health Organization, approximately 37 million people are currently living with HIV, with 1.8 million newly infected in 2017 alone.[1] While nucleoside reverse transcriptase inhibitors (NRTIs) have served as a cornerstone of highly active antiretroviral therapy (HAART) for HIV, novel drug classes are needed to improve drug adherence through improved safety, long-term efficacy, and simplified dosing regimens.[2] One particularly promising molecule is islatravir (**1**, EFdA or MK-8591), a long-acting nucleoside reverse transcriptase translocation inhibitor (NRTTI) that binds to the polymerase active site of HIV reverse transcriptase.[3] This investigational new drug has been shown to suppress HIV viral load for extended duration at low doses, opening the possibility of implantable formulations that have promising implications for drug adherence.[4]

A number of approaches to the total synthesis of islatravir (**1**) have been reported, including 22-step[5] and 18-step syntheses[6] from the Kuwaraha group and a 15-step synthesis from McLaughlin and co-workers.[7] Considering the recent clinical promise surrounding islatravir (**1**), we sought a more efficient synthesis to enable an inexpensive manufacturing scale supply. To this end, we recently disclosed a biocatalytic route to islatravir involving a highly efficient aldol-glycosylation one-pot biocatalytic cascade.[8] During the development of the biocatalytic route, we simultaneously explored alternative routes leveraging the highly efficient enzymatic glycosylation, but accessing key intermediates from chemocatalytic approaches.[9] Herein, we describe the shortest and highest yielding of these approaches enabled through a novel enantioselective alkynylation of an alpha-beta unsaturated ketone.[10]

Results and Discussion

Our retrosynthetic approach intercepts the biocatalytic cascade at the key intermediate, 2-ethynylglyceraldehyde-3-phosphate, **2**.

We proposed a general strategy of using an olefin as a masked aldehyde to cleanly reveal 2-ethynylglyceraldehyde-3-phosphate **2** via ozonolysis (Scheme 1). The chiral allylic alcohol precursor **3** could arise from an enantioselective alkynylation of an *α'*-phosphorylated-*α,β*-unsaturated ketone **4**, which, in turn, can be readily accessed from commodity chemicals. To accomplish the proposed route, we needed to develop an unprecedented enantioselective alkynylation, demonstrate a safe and selective ozonolysis, and understand the handling of highly functionalized and unstable intermediates.

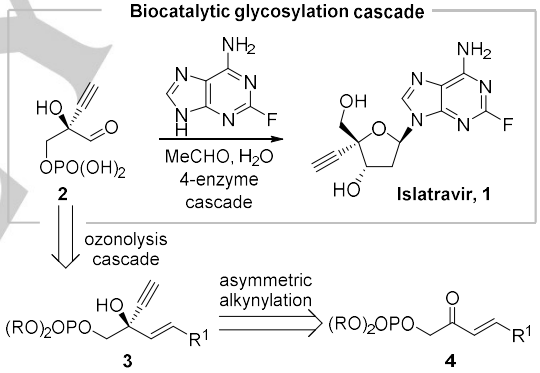

Scheme 1. Retrosynthetic approach to islatravir (**1**).

Recognizing the challenges associated with developing an asymmetric enone alkynylation, we prioritized the synthesis of a library of electronically and sterically diverse substrates at the outset. Benzylideneacetone derivatives were considered an attractive, inexpensive starting point since the *α'*-phosphorylated-*α,β*-unsaturated ketones could be accessed in two steps from commodity chemicals.[11] Electrophilic halogenation of electon-rich ketones (**5**),[12] or a Wittig olefination of electron-defficient aldehydes (**6**) using a commercially available ylide[13] provided the *α*-chloroketones that were readily converted to the *α*-phosphates (**4**) by an S_N2 reaction (Scheme 2).[14]

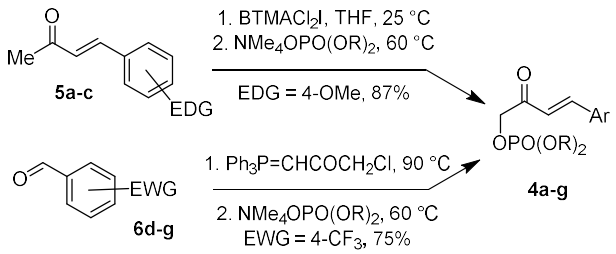

Scheme 2. Two-step access to *α*-phosphorylated benzalacetone derivatives. $BTMACl_2I$ = benzyltrimethylammonium dichloroiodate.

Investigation into the racemic alkynylation of the resulting ketones using ethynyl magnesium chloride (**7**) quickly revealed that the diethyl phosphate derivatives were unstable toward strongly nucleophilic conditions, while the bulky *tert*-butyl phosphates proceeded quantitatively (Table 1, **4a** vs **4b**).[15] Further advantages to employing *tert*-butyl phosphates are the ease of deprotection using mild acid (*vide infra*), and the unexpected observation that most of the *tert*-butyl phosphate containing compounds were crystalline solids. Less rigid alkyl phosphates (eg. **4a**) often exist as oils having implications on stability, as well as precluding bulk purification via recrystallization. Finally, we discovered that alkynylation of electron rich substrates provided products with improved stability which is reflected in the isolated yields compared to the NMR yields (**3c** vs **3g**).

Table 1. Racemic alkynylation of various *α*-phosphorylated ketones.

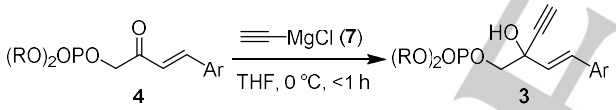

SM	Ar	R	allylic alcohol	yield[a]
4a	Ph	Et	**3a**	57 (65)
4b	Ph	^{t}Bu	**3b**[b]	96
4c	4-OMeC$_6$H$_4$	^{t}Bu	**3c**[b]	93
4d	naphthyl	^{t}Bu	**3d**	93
4e	4-FC$_6$H$_4$	^{t}Bu	**3e**	88
4f	4-CF$_3$C$_6$H$_4$	^{t}Bu	**3f**	81 (96)
4g	4-CNC$_6$H$_4$	^{t}Bu	**3g**	77 (93)

[a] Isolated yields shown with NMR assay yield in parenthesis. [b] Halogenation, phosphorylation and alkynylation run on > 400 g scale.

With a library of electronically diverse substrates with stability toward alkynylation designed into the structure, we pursued an enantioselective alkynylation. In contrast to the alkynylation of aldehydes, enantioselective alkynylation of ketones is more challenging, and efforts involving alkynylation of enones have only focused on 1,4-addition.[16] Accordingly, we evaluated a variety of ligands (via high-throughput experimentation) to induce enantioselective alkynylation of enone **4b** by ethynylmagnesium chloride (**7**). Chiral ligand classes explored include BINOLs and chiral diols, PyBox, salens and salans. Metal additives such as LiHMDS, ZnR_2 (R = Me, Et) and triflate salts were also screened.

Table 2. Identification of chiral ligand and reaction conditions

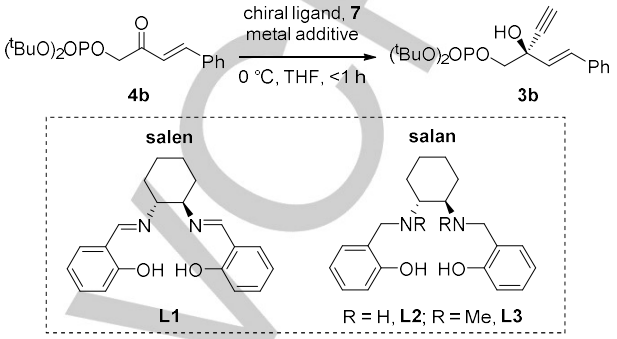

Entry	ligand	e.r.	conditions
1	**L1**	44:56	50 mol% **L1**, no metal additive
2	**L2**	42:58	50 mol% **L2**, 50 mol% LiHMDS
3	**L3**	79:21	50 mol% **L3**, 2 equiv **7**
4	**L3**	82:18	As entry 3, with 25 mol% LiHMDS
5	**L3**	77:23	As entry 4, ethynylMgBr instead of **7**
6	**L3**	69:31	As entry 4, toluene as solvent

>90% conversion to **3b** observed in all conditions shown in table.

Most ligand classes evaluated resulted in poor enantioselectivity and/or conversion (see SI), including salen ligands, which have previously been used in enantioselective alkynylation of ketones (Table 2, entry 1, **L1**).[16c, 17] While related reduced ligand **L2** provided similar enantioselectivity (Table 2, entry 2), the *N*-methyl salan ligand **L3** was identified as a promising lead, providing >95% conversion with 79:21 e.r., indicating the importance of the *N*-Me group on the ligand (Table 2, entry 3). Salan ligands incorporating the diaminocyclohexane backbone have previously been used for various asymmetric synthetic transformations, including organogallium or organozinc addition to aldehydes, when paired with metals such as Al, V, Zn, Ti, Nb and Zr.[18] LiHMDS as an additive resulted in higher er (Table 2, entry 4), but higher loadings led to an erosion in the product enantioselectivity (e.g. 64:36 er at 100 mol% LiHMDS). Additionally, the use of ethynylmagnesium bromide instead of the corresponding chloride (**7**) resulted in a lower e.r. (Table 2, entry 5). Use of 2-MeTHF or MTBE as solvent resulted in similar enantioselectivities, while the selectivity was worse in toluene, CF_3Ph and CPME (Table 1 and SI). Cooling the reaction to –20 °C failed to further improve the er.

We next investigated the impact of the substrate phenyl electronic properties upon the enantioselectivity of the product. The presence of electron-donating aryl groups led to higher enantioselectivities, with a negative Hammett correlation (Figure

1). The small magnitude of the ρ value indicates this is a minor effect: *para*-methoxy substitution (substrate **4c**) provided the highest enantioselectivity of 83:17 e.r. under these conditions, compared with 80:20 and 74:26 when R = Ph or CN, respectively.

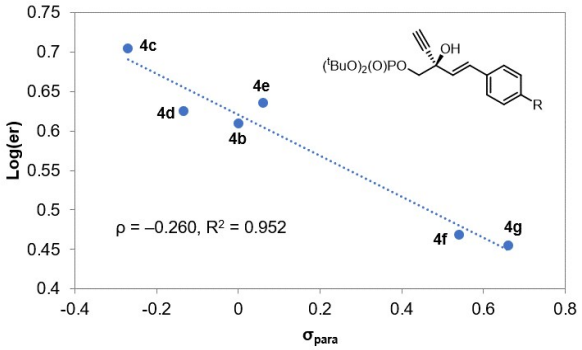

Figure 1. Hammett plot depicting enantiomeric ratio *vs* σ_{para} of the substrate. For point ***a***, aryl group = 2-naphthyl. Reactions conducted at 4 °C.

To explore the effect of the ligand upon the alkynylation of **4c**, modifications of **L1** were conducted. As observed in Jacobsen's Mn-salen-catalyzed epoxidation,[19] the electronic properties of the aryl group on the ligand played an important role in controlling the product enantioselectivity. The employment of electron-donating substituents on the 4-position of the phenol rings generally promoted higher enantioselectivities in the reaction (Table 3). *Ortho*- substituents (*e.g.* 2,4-di-Cl or 2,4-di-^{t}Bu substitution patterns) significantly decreased the er (Table 3 and SI), which may suggest dimer formation is required for catalysis and this process is hindered by the presence of steric bulk proximal to the metal (*vide infra*). The optimal combination of ligand **L4** with substrate **4c** achieved an er of 90:10 for alkynylated product **3c** (Table 3, entry 7).

Table 3. Effect of ligand electronics and reaction conditions upon the enantioselectivity of the alkynylation of **4c**

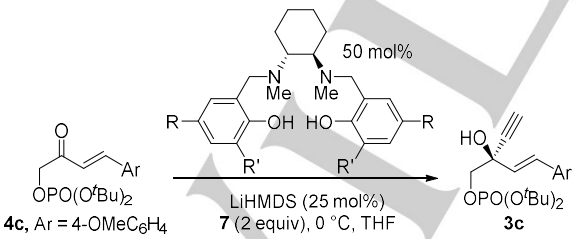

Entry	ligand	e.r.	conditions
1	R = H, R' = H (**L3**)	84:16	As above
2	R = Me, R' = H	84:16	As above
3	R = Cl, R' = H	74:26	As above
4	R = OMe, R' = H	86:14	As above
5	R = ^{t}Bu, R' = H (**L4**)	88:12	As above
6	R = ^{t}Bu, R' = ^{t}Bu	49:51	As above
7	**L4**	90:10	100 mol% **L4**; 50 mol% LiHMDS, 3 eq. **7**

We next sought a deeper mechanistic understanding of the new alkynylation reaction. Both the salan-mediated and racemic alkynylations of substrates **4b** and **4c** proceeded rapidly to >95% conversion within 30 seconds at 0 °C. Attempts to further cool the reaction to monitor kinetics were hampered by precipitation of the catalyst at ca. –30 °C. Although the reaction was too fast to monitor kinetics by conventional methods, clues into the nature of the alkynylation catalyst were provided by varying the amount of reagent **7** while holding **4b** (1 equiv), **L3** (0.5 equiv) and LiHMDS (0.25 equiv) constant. With 0.5 equiv **7**, no reaction was observed within 1 hour, but with 1 equiv, 13% conversion was observed in the same timeframe. With 1.5 equiv, 60% conversion was observed, and 2 equiv afforded complete conversion. These results suggest that, with 0.5 equiv **L3**, approximately 1 equiv of **7** is sequestered in catalyst formation, implying that the catalyst structure involves 2 Mg ions per salan.

To probe the involvement of the alkynyl group in catalyst formation, experiments were conducted in which different Grignard reagents were added sequentially to salan **L3** followed by exposure to the enone **4b** (Table 4). When R^1 = ethyl and R^2 = ethynyl (Table 4, Entry 3), the major product is alkynylation with a similar ee as when R^1 = R^2 = ethynyl (Table 4, Entry 1). This result suggests that the active catalyst is formed from the addition of R^1MgCl whether using EtMgCl or **7**. Entry 2 suggests that the Grignard reagent (**7**) is consumed mostly for complex formation, and then EtMgCl adds to the ketone. Importantly for scale-up considerations, utilization of EtMgCl instead of (**7**) for catalyst formation significantly improves the safety profile (avoiding liberation of acetylene gas), volumetric efficiency and cost of the catalyst formation step.[20]

Table 4. Mixed Grignard experiments

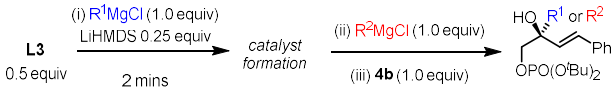

Entry	R^1	R^2	alkynylation[a] %	alkylation[a] %	alkynylation e.r.
1	Ethynyl	Ethynyl	100	-	79:21
2	Ethynyl	Ethyl	29	71	ND[b]
3	Ethyl	Ethynyl	93	7	79:21

[a] Relative % alkynylation vs alkylation shown, determined by SFC analysis. [b] Not determined due to overlapping side products in the SFC chromatogram.

A non-linear effect was observed in the alkynylation product ee when varying the ee of salan **L4** (Figure 2). Simulations of Kagan's ML_2 (or $(ML)_2$) model[21] fit the experimental data well, consistent with a dimeric catalyst species being involved in the

enantioselectivity-determining step. A similar non-linear effect was also observed with ligand **L3**. This observation is in contrast to V-salan catalyzed oxidation reactions,[18d] or Cozzi's Ti-salen catalyzed ketone alkynylation,[16c] in which monomeric catalyst species were proposed, although many other dimeric salen complexes have been used previously in asymmetric catalysis.[22]

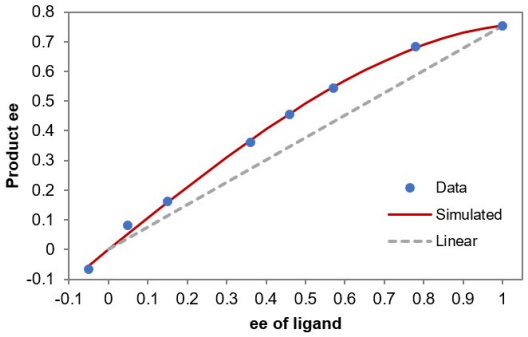

Figure 2. Non-linear effect using **L4** and Kagan's ML_2 model.

Consistent with the observed non-linear effect, crystallographic evidence of dimeric species was obtained: addition of LiHMDS and **7** in THF to ligand **L4**, followed by layering the solution with hexanes at 5 °C, yielded colorless single crystals suitable for X-ray diffraction. The solid-state structure of this complex (**8**, Figure 3) shows that two Mg centers, with approximate octahedral coordination geometry, are each coordinated to a salan ligand, and bridged by two Cl atoms. Two additional pentacoordinate Mg atoms (each bound to a chloride and THF molecule) bridge the phenoxy groups on opposing salan ligands. This structure is consistent with earlier results that implied a 2:1 Mg:salan ratio is required to form the alkynylating agent.[23] While many catalysts utilizing a salan ligand with the diaminocyclohexane backbone are proposed to operate as monomeric species (with supporting crystallographic evidence in several cases[18h, 24]), multimetallic or dimeric catalysts have also been reported.[18e, 25]

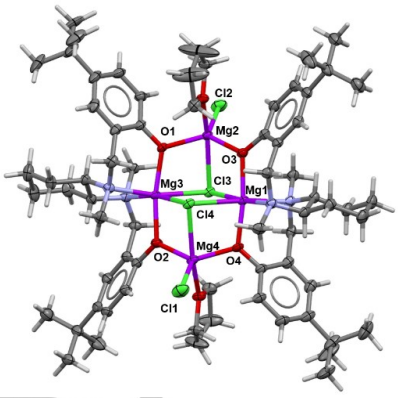

Figure 3. Solid-state structure of complex **8**. Displacement ellipsoids are shown at 50% probability.

The solution state NMR spectra of complex **8** are consistent with the solid-state structure. Two 1:1 sets of salan signals were observed, indicating the existence of two different conformations of salan subunits (as was observed in the solid-state structure, see SI), and both subunits featured a heavily shielded *N*-methine (δ $^{1}H/^{13}C$: 2.10/55.0, 1.63/66.0 ppm). NMR spectroscopy of freshly-made *in situ* salan/**7** mixtures shows peaks matching the predicted chemical shifts of complex **8** (see SI). This shows that LiHDMS is not required for formation of **8**. Several other species are present within the *in situ* formed catalyst mixture, assigned by DOSY experiment as dimers with similar molecular sizes to structure **8**. Upon addition of Li-based additives $LiBF_4$ or LiTMP (which give similar enantioselectivities as LiHMDS, Table 2), dimeric species (including complete **8**) remain, albeit with differing distributions/chemical shifts. While we cannot definitively rule out a monomeric active catalyst, the available evidence points to a dimeric active catalyst in which the coordination can be subtly influenced by lithium-based additives to provide a small increase in the e.r. of the obtained product. Moreover, the evidence is consistent with ethynyl magnesium bromide producing lower enantioselectivity than the corresponding chloride (**7**) for the alkynylation (*vide supra*) likely due to significant alterations to the dimeric catalyst structure when replacing chloride with bromide.

Under optimized conditions (3.75 equiv **7**, 0.90 equiv **L4**, and 0.57 equiv LiHMDS), 1 g of *α,β*-unsaturated ketone **4c** afforded chiral product **3c** in 96% yield and 90:10 er. With the enantioenriched allylic alcohol in hand, dealkylation of the *tert*-butyl groups and ozonolysis of the olefin would provide the desired 2-ethynylglyceraldehyde-3-phosphate (**2**). An initial investigation showed that the acidic conditions required to catalyze dealkylation of the phosphate also catalyzed the isomerization of the allylic alcohol to form a conjugated enyne (Scheme 3, **9**). Gratifyingly, reversal of the steps allowed for clean ozonolysis of the allylic alcohol to 2-ethynylglyceraldehyde-3-di-*tert*-butylphosphate, thus eliminating concerns around allylic transposition.[26] Unsurprisingly, the aldehyde generated from ozonolysis was found to be unstable in organic solvents, but readily formed a stabilized hydrate in aqueous solvents. Difficulty in isolating the di-*tert*-butylphosphate due to decomposition via phosphate ester migration (Scheme 3, **10**) guided us toward the goal of developing a one-pot procedure to convert allylic alcohol **3c** directly to hydrate **2**.

Drawing inspiration from Dussault and Molander,[27] we viewed ozonolysis in water with an acetone co-solvent as optimal for our purposes. In addition to the aqueous conditions stabilizing hydrate **2** (see Scheme 3, **11**), the safe mixed solvent system emerged as a rare combination that served to solubilize both starting material **3c** and product **2**. Indeed, a 9:1 mixture of acetone-water enabled creation of a homogeneous reaction mixture throughout the course of the transformation, and no ozonides were detected at any point during the reaction. Furthermore, we were pleased to observe that dealkylation of the phosphate was spontaneous and autocatalytic after the Me_2S quench. Upon revealing the free phosphate, addition of pentanes allowed for separation of the acetone layer containing the majority of the byproducts leaving only 0.8 equiv of DMSO and 1.5 equiv of ^{t}BuOH in the remaining aqueous solution, containing hydrate **2** in 93% yield.

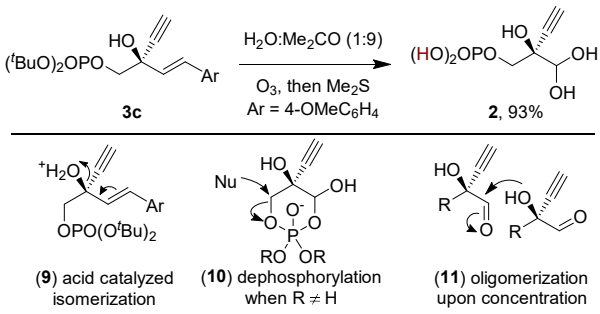

Scheme 3. Ozonolysis of allylic alcohol **3c** and side reactions avoided by using an aqueous cascade protocol.

Because of the high concentration (up to 0.4 M) and high purity of the ozonolysis reaction stream, isolation of the product as a calcium salt was possible simply by addition of $Ca(OAc)_2$ followed by ^{i}PrOH trituration.[28] Although isolation enabled good purity control at the penultimate step, it was deemed unnecessary as our ozonolysis crude stream could be used directly in the aldol-glycosylation cascade more effectively then when contaminated by calcium salts.[29] In fact, the high purity and concentration of intermediate **2** from the ozonolysis stream allowed the synthesis to be completed with more favorable conditions and higher yield than reported in our previous fully biocatalytic approach (82% vs 76%) (Table 5).[8]

Table 5. Stereospecifity of the biocatalytic aldol-glycosylation cascade.

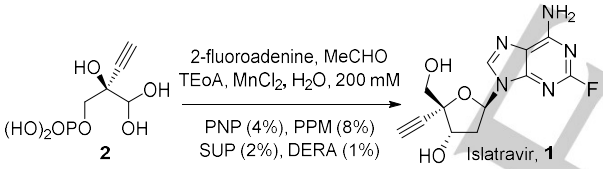

e.r. of **3**[a]	e.r. of API	d.r. of API	yield of **1**[b]	overall yield [c]
99:1	>99:1	>99:1	82	47[d]
50:50	>99:1	>99:1	44	32
90:10	>99:1	>99:1	74	54

[a] er was determined for the alkynylation products and API, but not for **2**. [b] Isolated yield for the aldol-glycosylation cascade vs **2**. Yields vs. the limiting reagent (2-FA is 0.85 equiv) are ≥ 93% in all cases (see SI). [c] Isolated yield of the entire route from anisylidene acetone. [d] An upgrade from 90:10 e.r. to 99:1 e.r. of **3c** can be achieved by recrystallization from MeCN/H2O in 78% recovery. DERA = deoxyribose aldolase, PNP = purine nucleoside phosphorylase, PPM = phosphopentamutase, SUP = sucrose phosphorylatse, TEoA = triethanolamine.

The enzymatic cascade was shown to be completely stereoselective providing islatravir as a single isomer independent of the enantiomeric purity of the incoming substrate (Table 5). A comparison of overall yields shows that, while discarding >50% of the substrate in the final step can be accomplished, it severely affects the overall efficiency of the route, as expected. However, the 90:10 e.r. obtained in the alkynylation approach is not only acceptable for delivering high ee product, but actually provides a higher overall yield (54% vs. 47%) than recrystallizing at an earlier stage.[30] The unique ability to carry through imperfect enantiomeric ratios and eliminate time and material-consuming recrystallization steps highlights a less obvious advantage of employing highly specific biocatalytic cascades late in a synthesis.[31]

Conclusion

In conclusion, we have developed a 5-step asymmetric synthesis of islatravir (**1**) from commodity chemicals. To achieve this goal, a novel reaction involving the asymmetric alkynylation of an *α'*-phosphorylated-*α,β*-unsaturated ketone and an ozonolysis-dealkylation cascade were developed. Finally, an enzymatic aldol-glycosylation cascade was leveraged to construct the desired bonds with complete stereoselectivity regardless of the enatiomeric purify of the penultimate, highlighting the power of late stage biocatalytic transformations.

Acknowledgements

Thanks to Yafei Li (Pharmaron, Inc.) for assistance with ligand synthesis.

Keywords: synthesis • asymmetric alkynylation • ozonolysis • biocatalysis •

[1] HIV Surveillance Supplemental Report 2017; 22(No. 2). http://www.cdc.gov/hiv/library/reports/hivsurveillance.html. Published July 2017. Accessed Oct 22, 2019.

[2] a) M. P. de Bethune, *Antiviral Res.* **2010**, *85*, 75-90; b) D. G. Prajapati, R. Ramajayam, M. R. Yadav, R. Giridhar, *Bioog. Med. Chem.* **2009**, *17*, 5744-5762; c) C. Flexner, *Nat. Rev. Drug Discovery* **2007**, *6*, 959-966.

[3] a) E. Michailidis, A. D. Huber, E. M. Ryan, Y. T. Ong, M. D. Leslie, K. B. Matzek, K. Singh, B. Marchand, A. N. Hagedorn, K. A. Kirby, L. C. Rohan, E. N. Kodama, H. Mitsuya, M. A. Parniak, S. G. Sarafianos, *J. Biol. Chem.* **2014**, *289*, 24533-24548; b) H. Ohrui, *Chem. Rec.* **2006**, *6*, 133-143; c) S. Kohgo, K. Yamada, K. Kitano, Y. Iwai, S. Sakata, N. Ashida, H. Hayakawa, D. Nameki, E. Kodama, M. Matsuoka, H. Mitsuya, H. Ohrui, *Nucleosides, Nucleotides Nucleic Acids* **2004**, *23*, 671-690.

[4] a) C. A. Stoddart, S. A. Galkina, P. Joshi, G. Kosikova, M. E. Moreno, J. M. Rivera, B. Sloan, A. B. Reeve, S. G. Sarafianos, M. Murphey-Corb, M. A. Parniak, *Antimicrob. Agents Chemother.* **2015**, *59*, 4190-4198; b) S. E. Barrett, R. S. Teller, S. P. Forster, L. Li, M. A. Mackey, D. Skomski, Z. Yang, K. L. Fillgrove, G. J. Doto, S. L. Wood, J. Lebron, J. A. Grobler, R. I. Sanchez, Z. Liu, B. Lu, T. Niu, L. Sun, M. E. Gindy, *Antimicrob. Agents Chemother.* **2018**, *62*, e01058-18.

[5] K. Fukuyama, H. Ohrui, S. Kuwahara, *Org. Lett.* **2015**, *17*, 828-831.

[6] a) M. Kageyama, T. Miyagi, M. Yoshida, T. Nagasawa, H. Ohrui, S. Kuwahara, *Biosci., Biotechnol., Biochem.* **2012**, *76*, 1219-1225; b) M. Kageyama, T. Nagasawa, M. Yoshida, H. Ohrui, S. Kuwahara, *Org. Lett.* **2011**, *13*, 5264-5266.

[7] M. McLaughlin, J. Kong, K. M. Belyk, B. Chen, A. W. Gibson, S. P. Keen, D. R. Lieberman, E. M. Milczek, J. C. Moore, D. Murray, F. Peng, J. Qi, R. A. Reamer, Z. J. Song, L. Tan, L. Wang, M. J. Williams, *Org. Lett.* **2017**, *19*, 926-929.

[8] Huffman, M. A.; Fryszkowska, A.; Alvizo, O; Borra-Garske, M.; Campos, K. R.; Canada, K. A.; Devine, P. N.; Duan, Da.; Forstater, J. H.; Grosser, S. T.; Halsey, H. M.; Hughes, G. J.; Jo, J.; Joyce, L. A.; Kolev, J. N.; Liang, J.; Maloney, K. M.; Mann, B. F.; Marshall, N. M.; McLaughlin, M.; Moore, J. C.; Murphy, G. S.; Nawrat, C. C.; Nazor, J.; Novick, S.; Patel, N. R.; Rodriguez-Granillo, A.; Robaire, S. A.; Sherer, E.; Truppo, M. D.; Whittaker, A. M.; Verma, D.; Xiao, L.; Xu, Y.; Yang, H. *Science* **2019**, *366*, 1255–1259.

[9] a) N. R. Patel, C. C. Nawrat, M. McLaughlin, Y. Xu, M. A. Huffman, H. Yang, H. Li, A. M. Whittaker, T. Andreani, F. Lévesque, A. Fryszkowska, A. Brunskill, D. M. Tschaen, K. M. Maloney, *Org. Lett.* **2020**, *22*, 4659-4664; b) C. C. Nawrat, A. M. Whittaker, M. A. Huffman, M. McLaughlin, R. D. Cohen, T. Andreani, B. Ding, H. Li, M. Weisel, D. M. Tschaen, *Org. Lett.* **2020**, *22*, 2167-2172.

[10] In addition to the higher yield and shorter step count, reference 8-9 begin from custom materials. The synthesis described herein starts from commodity chemicals available in multi-ton quantities.

[11] a) Y. Yang, C. Qu, X. Chen, K. Sun, L. Qu, W. Bi, H. Hu, R. Li, C. Jing, D. Wei, S. Wei, Y. Sun, H. Liu, Y. Zhao, *Org. Lett.* **2017**, *19*, 5864-5867; b) C. Sun, R. Bittman, *J. Org. Chem.* **2004**, *69*, 7694-7699.

[12] P. B. Huleatt, M. L. Khoo, Y. Y. Chua, T. W. Tan, R. S. Liew, B. Balogh, R. Deme, F. Goloncser, K. Magyar, D. P. Sheela, H. K. Ho, B. Sperlagh, P. Matyus, C. L. Chai, *J. Med. Chem.* **2015**, *58*, 1400-1419.

[13] K. S. Babu, X. C. Li, M. R. Jacob, Q. Zhang, S. I. Khan, D. Ferreira, A. M. Clark, *J. Med. Chem.* **2006**, *49*, 7877-7886.

[14] B. Zheng, R. J. Fox, M. Sugiyama, A. Fritz, M. D. Eastgate, *Org. Process Res. Dev.* **2014**, *18*, 636-642.

[15] V. R. Sabbasani, H. Lee, Y. Xia, D. Lee, *Angew. Chem. Int. Ed. Engl.* **2016**, *55*, 1151-1155.

[16] a) B. M. Trost, A. H. Weiss, *Adv. Synth. Catal.* **2009**, *351*, 963-983; b) T. Bauer, *Coord. Chem. Rev.* **2015**, *299*, 83-150; c) P. G. Cozzi, *Angew. Chem.* **2003**, *115*, 3001-3004; d) Y. Zheng, Y. Tan, K. Harms, M. Marsch, R. Riedel, L. Zhang, E. Meggers, *J. Am. Chem. Soc.* **2017**, *139*, 4322-4325; e) B. Bieszczad, D. G. Gilheany, *Angew. Chem. Int. Ed. Engl.* **2017**, *56*, 4272-4276.

[17] D. Park, C. I. Jette, J. Kim, W. O. Jung, Y. Lee, J. Park, S. Kang, M. S. Han, B. M. Stoltz, S. Hong, *Angew. Chem. Int. Ed. Engl.* **2020**, *59*, 775-779.

[18] a) H. Du, A. H. Velders, P. J. Dijkstra, J. Sun, Z. Zhong, X. Chen, J. Feijen, *Chem. Eur. J.* **2009**, *15*, 9836-9845; b) A. Yeori, I. Goldberg, M. Shuster, M. Kol, *J. Am. Chem. Soc.* **2006**, *128*, 13062-13063; c) J. Sun, Z. Dai, M. Yang, X. Pan, C. Zhu, *Synthesis* **2008**, *2008*, 2100-2104; d) J. Sun, C. Zhu, Z. Dai, M. Yang, Y. Pan, H. Hu, *J. Org. Chem.* **2004**, *69*, 8500-8503; e) H. Egami, T. Katsuki, *Angew. Chem. Int. Ed.* **2008**, *47*, 5171-5174; f) Z. Dai, M. Shao, X. Hou, C. Zhu, Y. Zhu, Y. Pan, *Appl. Organomet. Chem.* **2005**, *19*, 898-902; g) Z. Dai, C. Zhu, M. Yang, Y. Zheng, Y. Pan, *Tetrahedron: Asymmetry* **2005**, *16*, 605-608; h) A. Yeori, S. Groysman, I. Goldberg, M. Kol, *Inorg. Chem.* **2005**, *44*, 4466-4468.

[19] E. N. Jacobsen, W. Zhang, M. L. Guler, *J. Am. Chem. Soc.* **1991**, *113*, 6703-6704.

[20] **7** is available as a 0.5 M THF solution at $154 / 800 mL, while EtMgCl is available as a 2 M THF solution at $226 / 800 mL (www.sigmaaldrich.com on Nov 8th 2019). Therefore, catalyst formation with the more concentrated EtMgCl represents cost and volume reductions, which are important considerations on scale.

[21] D. Guillaneux, S.-H. Zhao, O. Samuel, D. Rainford, H. B. Kagan, *J. Am. Chem. Soc.* **1994**, *116*, 9430-9439.

[22] S. Shaw, J. D. White, *Chem. Rev.* **2019**, *119*, 9381-9426.

[23] The crystals of **8** were formed amongst oils and LiOH/$Mg(OH)_2$, so were not clean enough to be used directly as a catalyst.

[24] H. Elias, F. Stock, C. Rohr, *Acta Cryst. C* **1997**, *53*, 862-864.

[25] D. A. Atwood, J. A. Jegier, K. J. Martin, D. Rutherford, *Organometallics* **1995**, *14*, 1453-1460.

[26] a) S. Goswami, A. K. Adak, *Tetrahedron Lett.* **2002**, *43*, 503-505; b) R. Persky, A. Albeck, *J. Org. Chem.* **2000**, *65*, 5632-5638; c) D. R. Edwards, C. T. Liu, G. E. Garrett, A. A. Neverov, R. S. Brown, *J. Am. Chem. Soc.* **2009**, *131*, 13738-13748.

[27] a) R. Willand-Charnley, T. J. Fisher, B. M. Johnson, P. H. Dussault, *Org. Lett.* **2012**, *14*, 2242-2245; b) C. E. Schiaffo, P. H. Dussault, *J. Org. Chem.* **2008**, *73*, 4688-4690; c) G. A. Molander, D. J. Cooper, *J. Org. Chem.* **2007**, *72*, 3558-3560.

[28] a) D. Gauss, B. Schoenenberger, R. Wohlgemuth, *Carbohydr. Res.* **2014**, *389*, 18-24; b) M. Binczarski, J. Berlowska, A. Stanishevsky, I. Witonska, *RSC Adv.* **2016**, *6*, 92420-92427.

[29] a) K. Hammer-Jespersen, A. Munch-Petersen, *Eur. J. Biochem.* **1970**, *17*, 397-407; b) T. D. Panosian, D. P. Nannemann, G. R. Watkins, V. V. Phelan, W. H. McDonald, B. E. Wadzinski, B. O. Bachmann, T. M. Iverson, *J. Biol. Chem.* **2011**, *286*, 8043-8054.

[30] See SI for details.

[31] In our previous report (reference 8) we obtained high ee of the product from high ee **2**. This is the first demonstration of a resolution using the same glycosylation cascade.

10.1002/chem.202003091

Entry for the Table of Contents

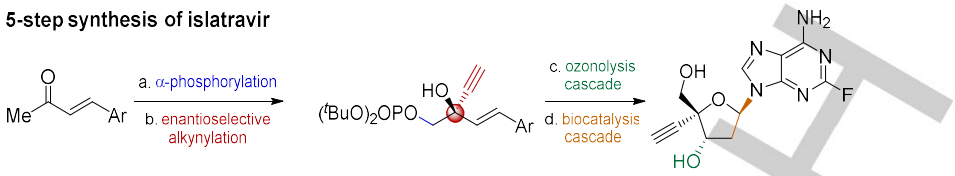

A 5-step enantioselective synthesis of the potent anti-HIV nucleoside islatravir is reported. The highly efficient route was enabled by a novel enantioselective alkynylation of an α,β-unsaturated ketone, a unique ozonolysis-dealkylation cascade in water, and an enzymatic aldol-glycosylation cascade.